SUPPLEMENTARY INFORMATION

Enhanced tonic $GABA_A$ inhibition in typical absence epilepsy

David W. Cope, Giuseppe Di Giovanni, Sarah J. Fyson, Gergely Orbán, Adam C. Errington, Magor L. Lorincz, Timothy M. Gould, David A. Carter and Vincenzo Crunelli.

Contents

SUPPLEMENTARY FIGURES

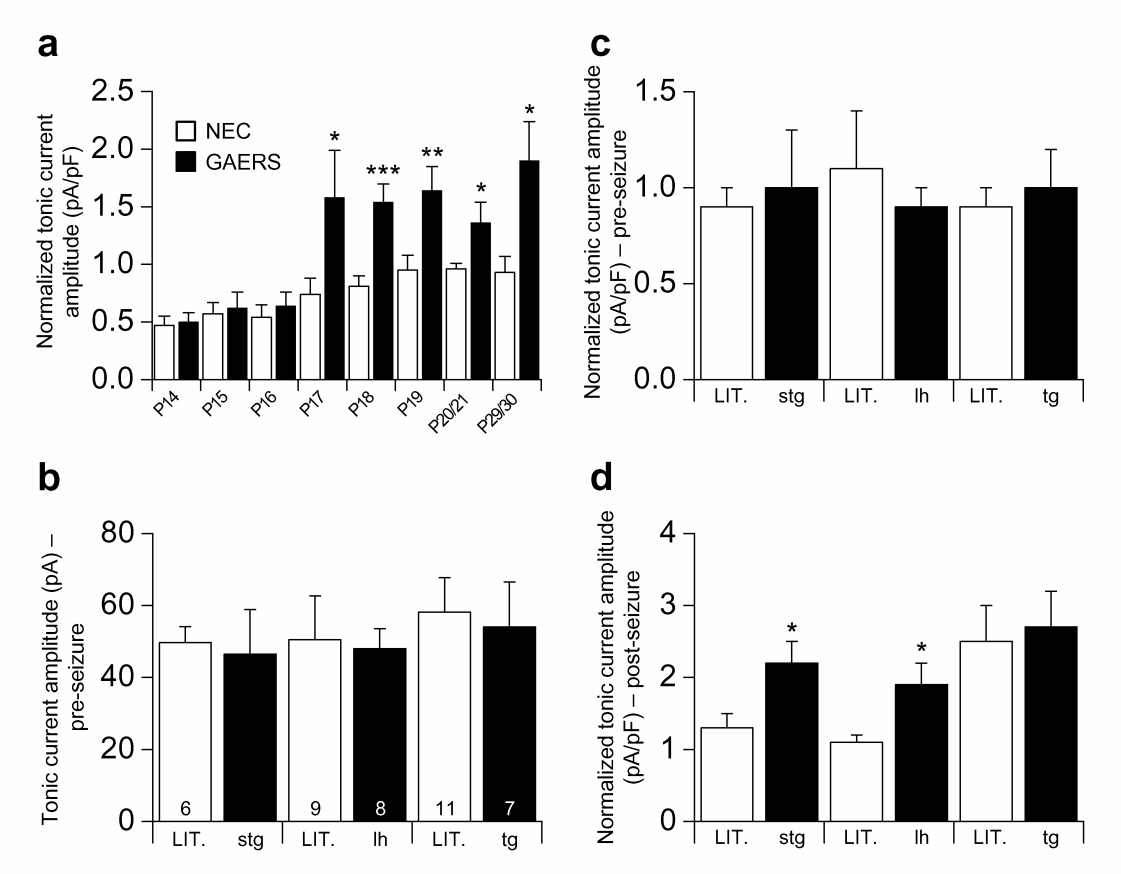

Supplementary Figure 1. Absolute and normalized tonic current amplitudes in TC neurons of GAERS and monogenic mutant mice. (**a**) Comparison of the normalized tonic current amplitude in NEC and GAERS for the same cells as in **Fig. 1b**. (**b**) Comparison of tonic current amplitude in pre–seizure stargazer (stg, P13–15, light grey column), lethargic (lh, P13–15, grey column) and tottering (tg, P16–18, dark grey column) mice compared to respective control littermates (LIT., white columns) of the same age. Number of recorded neurons are as indicated. (**c**) Comparison of normalized tonic current amplitude for the same neurons as in (**b**). (**d**) Normalized tonic current amplitude in post-seizure stargazer (P19–21), lethargic (P27–30) and tottering (P26–28) mice compared to respective control littermates (LIT.) of the same age. Number of recorded neurons are the same as indicated in **Fig. 1c**. * $P < 0.05$, ** $P < 0.01$, *** $P < 0.001$.

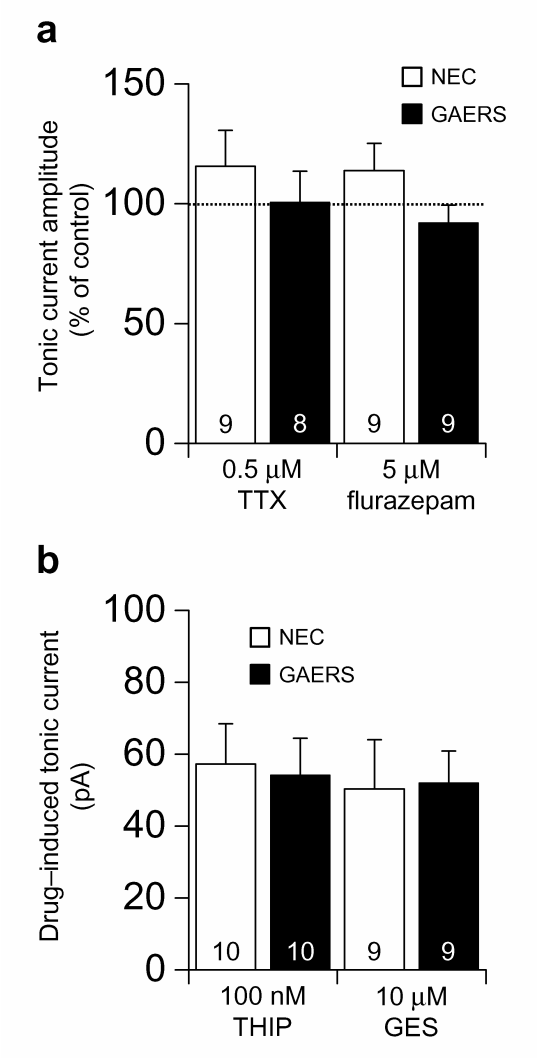

Supplementary Figure 2. Lack of contribution of non–GAT–1–dependent mechanisms to enhanced tonic current in GAERS. (**a**) Comparison of the effects of bath application of 0.5 µM TTX, and 5 µM flurazepam on tonic current amplitude in NEC and GAERS. Values were normalised to the average tonic current amplitude under control conditions. (**b**) Comparison of the drug–induced tonic current in NEC and GAERS following bath application of 100 nM THIP and 10 µM GES. Number of recorded neurons are as indicated.

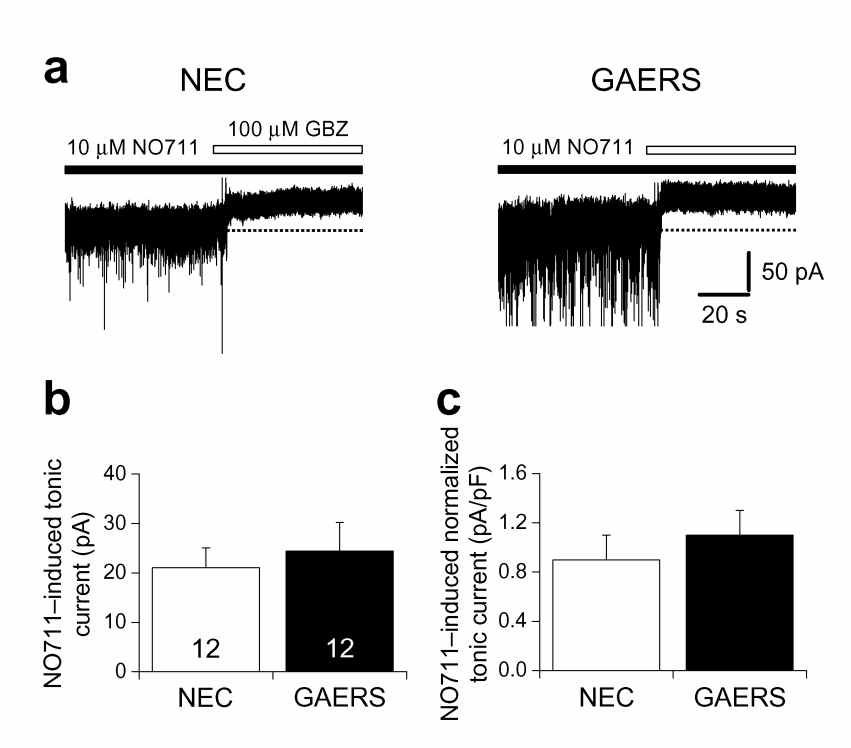

Supplementary Figure 3. GAT–1 activity is unaffected in DGGCs of GAERS. (**a**) Representative traces from P18–21 DGGCs of NEC (left) and GAERS (right) in the presence of the GAT–1 blocker NO711 (10 μM). Tonic currents were revealed by the focal application of 100 μM GBZ (white bars). (**b**) Comparison of the effect of NO711 on tonic current in NEC (white column) and GAERS (black column). Number of recorded neurons are as indicated. (**c**) Comparison of normalized tonic current amplitude following application of NO711 for the same neurons as in (**b**). Values in (**b**) and (**c**) were not significantly different.

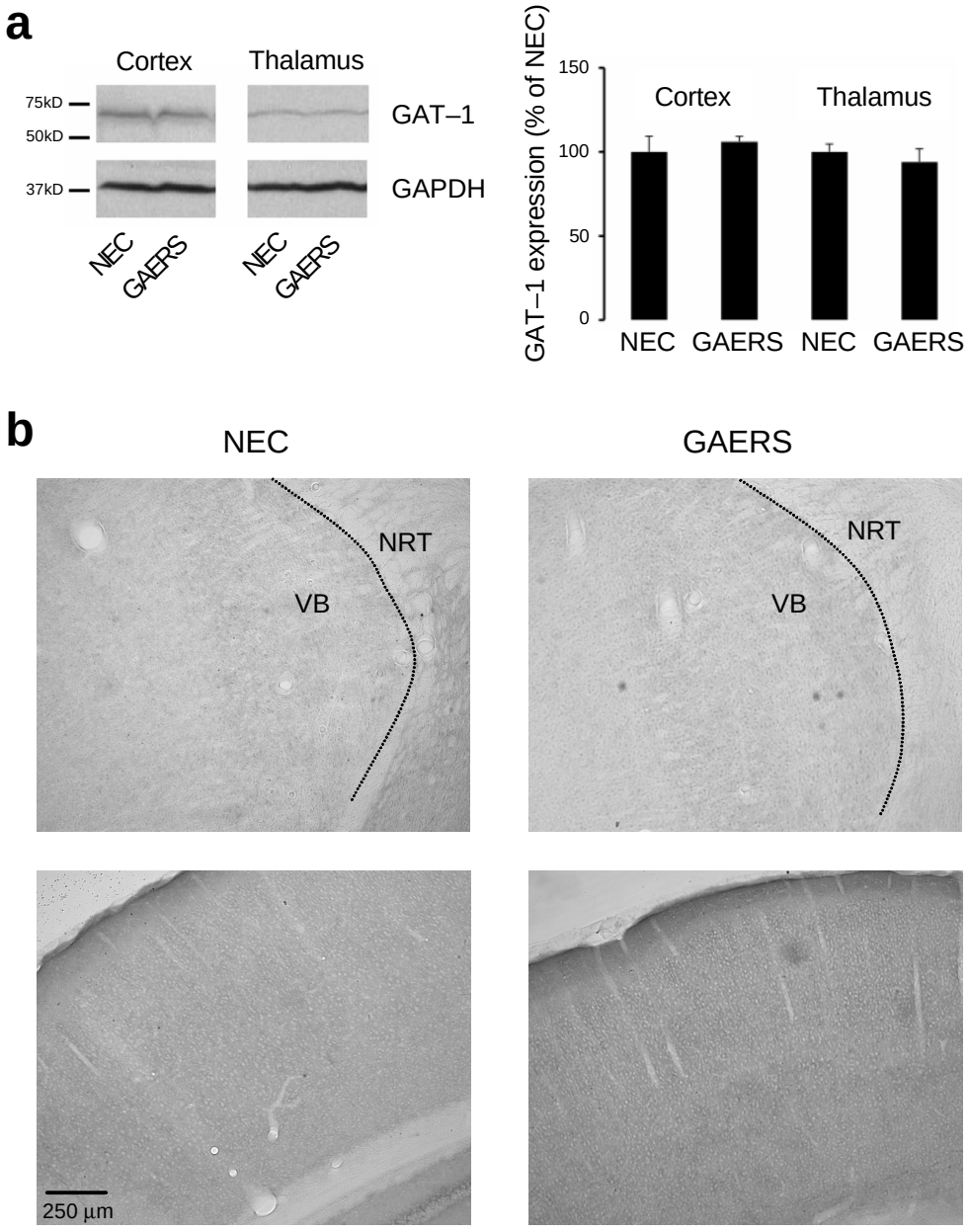

Supplementary Figure 4. GAT–1 expression is unaltered in GAERS. (**a**) Western blots (left) and quantitative comparison (right) of the relative levels of GAT–1 in cortex and thalamus of GAERS and NEC. (**b**) Immunohistochemical comparison of the expression of GAT–1 in perfusion-fixed thalamus (top) and neocortex (bottom) of NEC (left) and GAERS (right). Note the low level of expression in the thalamus compared to the cortex, and lack of difference in intensity in both strains. Dotted lines indicate the boundary between VB and the nucleus reticularis thalami (NRT).

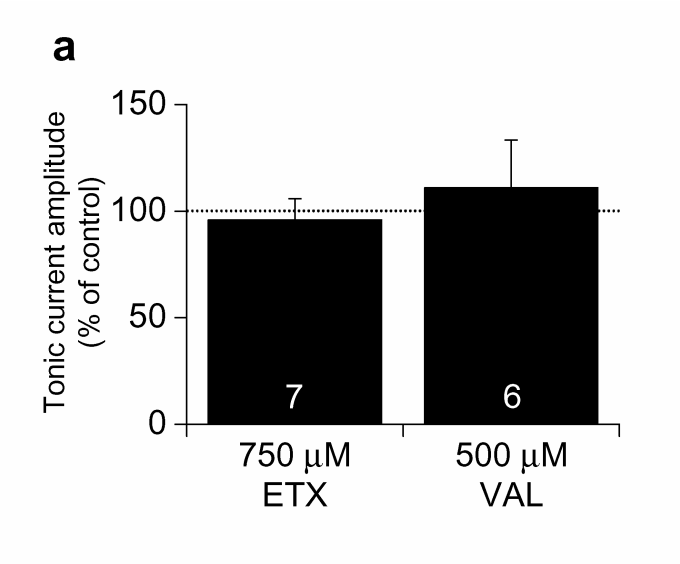

Supplementary Figure 5. The anti–absence drugs ethosuximide and sodium valrpoate do not affect tonic current amplitude in GAERS. (**a**) Effect of 750 μM ethosuximide (ETX) and 500 μM sodium valproate (VAL) on tonic current amplitude in TC neurons of P18–21 GAERS. Values were normalised to the average tonic current amplitude under control conditions. Number of recorded neurons for each drug are as indicated.

SUPPLEMENTARY TABLES

Rat strain and age		sIPSC parameter					
		n	Peak amplitude (pA)	Weighted decay (ms)	Frequency (Hz)	Charge transfer (fC)	Total current (pA)
P14	NEC	(14)	–52.7 ± 2.5	3.3 ± 0.3	8.0 ± 1.1	–193.6 ± 20.4	–1.5 ± 0.2
	GAERS	(13)	–53.6 ± 4.3	3.6 ± 0.2	4.5 ± 0.7 *	–222.2 ± 23.0	–1.1 ± 0.3
P15	NEC	(8)	–49.8 ± 3.2	2.6 ± 0.2	6.7 ± 1.1	–151.7 ± 14.7	–1.0 ± 0.2
	GAERS	(8)	–52.2 ± 4.3	2.5 ± 0.2	4.9 ± 0.9	–149.1 ± 15.6	–0.8 ± 0.1
P16	NEC	(10)	–55.9 ± 5.0	2.8 ± 0.2	5.7 ± 1.1	–174.1 ± 13.3	–1.0 ± 0.2
	GAERS	(9)	–42.1 ± 3.2 *	2.9 ± 0.2	4.2 ± 0.8	–138.8 ± 11.4	–0.6 ± 0.2
P17	NEC	(11)	–48.0 ± 5.0	2.8 ± 0.1	4.4 ± 0.8	–150.8 ± 17.0	–0.8 ± 0.2
	GAERS	(9)	–57.4 ± 6.1	3.2 ± 0.3	3.7 ± 0.9	–209.5 ± 28.8	–0.8 ± 0.3
P18	NEC	(9)	–58.1 ± 5.1	2.8 ± 0.2	6.6 ± 1.3	–191.9 ± 19.2	–1.3 ± 0.3
	GAERS	(12)	–42.5 ± 4.6 *	2.6 ± 0.1	3.6 ± 0.7 *	–124.6 ± 11.3 **	–0.5 ± 0.1 *
P19	NEC	(10)	–45.0 ± 4.7	2.5 ± 0.2	5.3 ± 1.3	–125.1 ± 9.8	–0.8 ± 0.2
	GAERS	(9)	–44.3 ± 3.9	2.1 ± 0.1	5.3 ± 2.2	–109.6 ± 10.2	–0.7 ± 0.4
P20/21	NEC	(13)	–37.9 ± 4.0	2.2 ± 0.1	2.8 ± 0.8	–93.8 ± 10.3	–0.3 ± 0.2
	GAERS	(14)	–41.6 ± 3.6	2.4 ± 0.2	3.8 ± 1.0	–117.8 ± 13.3	–0.5 ± 0.1
P29/30	NEC	(9)	–42.1 ± 6.4	2.1 ± 0.2	3.2 ± 0.5	–106.3 ± 24.3	–0.4 ± 0.1
	GAERS	(12)	–37.4 ± 2.8	2.7 ± 0.3	2.2 ± 0.7	–118.4 ± 19.0	–0.3 ± 0.1

Supplementary Table 1. Comparison of sIPSC properties in TC neurons of NEC and GAERS. Data are mean ± s.e.m. and *n* = number of recorded neurons. * $P < 0.05$ and ** $P < 0.01$.

Mouse strain and age	sIPSC parameter					
	n	Peak amplitude (pA)	Weighted decay (ms)	Frequency (Hz)	Charge transfer (fC)	Total current (pA)
P13-15 littermates	(6)	–34.9 ± 2.3	3.0 ± 0.2	6.3 ± 0.6	–115.5 ± 7.0	–0.7 ± 0.1
stargazer	(8)	–34.6 ± 1.3	3.7 ± 0.5	4.7 ± 0.7	–145.0 ± 25.7	–0.7 ± 0.2
P19-21 littermates	(13)	–44.7 ± 3.7	3.0 ± 0.4	6.7 ± 1.2	–147.4 ± 20.1	–1.1 ± 0.3
stargazer	(11)	–54.1 ± 5.8	3.1 ± 0.3	6.9 ± 0.9	–183.7 ± 24.6	–1.4 ± 0.3
P13-15 littermates	(10)	–44.7 ± 4.1	3.5 ± 0.4	7.5 ± 1.7	–172.2 ± 27.1	–1.3 ± 0.3
lethargic	(8)	–40.9 ± 2.7	3.0 ± 0.1	9.7 ± 2.4	–140.2 ± 10.6	–1.4 ± 0.5
P27-30 littermates	(10)	–58.1 ± 3.5	2.8 ± 0.3	8.7 ± 1.4	–180.9 ± 21.6	–1.4 ± 0.2
lethargic	(11)	–54.8 ± 4.1	2.2 ± 0.1	10.5 ± 2.5	–135.6 ± 11.0	–1.4 ± 0.4
P16-18 littermates	(12)	–41.7 ± 3.6	2.3 ± 0.2	5.1 ± 1.1	–105.3 ± 9.4	–0.6 ± 0.2
tottering	(7)	–37.8 ± 3.3	2.6 ± 0.1	5.9 ± 1.2	–110.2 ± 12.8	–0.7 ± 0.1
P26-28 littermates	(11)	–52.7 ± 2.6	1.9 ± 0.1	9.3 ± 2.2	–112.4 ± 8.1	–1.1 ± 0.3
tottering	(8)	–61.8 ± 5.0	1.9 ± 0.1	9.8 ± 2.1	–135.5 ± 15.7	–1.4 ± 0.5

Supplementary Table 2. Comparison of sIPSC properties in TC neurons of stargazer, lethargic and tottering mice, and respective control littermates. Data are mean ± s.e.m. and *n* = number of recorded neurons.

Cell type, strain and age	sIPSC parameter					
	n	Peak amplitude (pA)	Weighted decay (ms)	Frequency (Hz)	Charge transfer (fC)	Total current (pA)
TC neurons						
P68-74 WT	(9)	–58.4 ± 4.6	1.9 ± 0.1	7.9 ± 2.5	–121.2 ± 10.2	–1.0 ± 0.3
GAT-1 KO	(7)	–75.3 ± 6.9*	1.7 ± 0.2	21.7 ± 6.8*	–153.8 ± 28.0	–2.8 ± 0.8*
P23-30 WT	(5)	–80.3 ± 41.6	2.0 ± 0.4	4.9 ± 1.5	–145.1 ± 43.3	–0.7 ± 0.3
δ KO	(6)	–47.5 ± 3.5	1.9 ± 0.1	15.4 ± 4.3*	–103.4 ± 7.0	–1.6 ± 0.5
P28-32 GAERS						
Control	(10)	–43.2 ± 2.2	2.7 ± 0.3	5.8 ± 1.4	–128.4 ± 9.5	–0.7 ± 0.2
Missense	(8)	–42.2 ± 4.4	2.5 ± 0.4	5.3 ± 1.3	–129.4 ± 29.0	–0.6 ± 0.2
Antisense	(7)	–49.3 ± 5.6	2.8 ± 0.3	5.4 ± 1.5	–150.7 ± 31.5	–0.8 ± 0.2
DGGCs						
P18-21 NEC	(5)	–49.5 ± 2.9	5.0 ± 0.4	4.2 ± 1.3	–258.9 ± 24.4	–1.0 ± 0.3
GAERS	(5)	–62.2 ± 12.0	5.1 ± 1.0	3.3 ± 0.5	–373.3 ± 160.8	–1.3 ± 0.6

Supplementary Table 3. Comparison of sIPSC properties in TC neurons of GAT–1 KO and δ KO mice, and respective wildtype littermates (WT); TC neurons of GAERS under control conditions and following intra–thalamic administration of 2 nmol site^{-1} missense or 2 nmol site^{-1} δ subunit–specific antisense ODNs; and DGGCs of NEC and GAERS under control conditions. Data are mean ± s.e.m. *n* = number of recorded neurons. * $P < 0.05$.

LEGENDS FOR SUPPLEMENTARY MOVIES 1 AND 2

Supplementary Movie 1. Movie showing the occurrence of absence seizures in a normal Wistar rat during the intra–thalamic administration of 200 μM NO711. Note the strict time correlation between the behavioural components of the seizures (immobility and twitching of the vibrissae) and the appearance of large amplitude SWDs in the EEG, as depicted on the oscilloscope.

Supplementary Movie 2. Movie showing the occurrence of a number of absence seizures induced by the intra–thalamic administration of 100 μM THIP in a normal Wistar rat. The appearance of SWDs in the EGG correlates with the behavioural components of the seizures, including immobility, head and neck jerks, and twitching of vibrissae. Note the lack of head and neck jerks during the first seizure.

SUPPLEMENTARY RESULTS

Normalized tonic current amplitude in genetic models of typical absence seizures

We normalized tonic current amplitude to whole–cell capacitance to determine whether increased tonic current was due to changes in the basic cellular properties of the TC neurons. No difference in normalized tonic current amplitude between GAERS and NEC was observed from P14–16, but at P17 normalized tonic current amplitude became significantly larger in GAERS ($P < 0.05$). This increase was sustained in subsequent days (**Supplementary Fig. 1a**). No difference in normalized tonic current amplitude was observed between control littermates and stargazer, lethargic and tottering mice at pre–seizure ages (**Supplementary Fig. 1c**). However, normalized tonic current was significantly larger in post–seizure stargazer and lethargic (both $P < 0.05$), but not tottering, mice (**Supplementary Fig. 1d**), although the magnitude of the normalized tonic current in tottering mice was similar to both stargazer and lethargic. Importantly, there was no difference in whole–cell capacitance between any of the mutant and control strains at any age tested (data not shown).

Other cellular mechanisms do not contribute to enhanced tonic current in GAERS

Since tonic current in TC neurons is dependent on vesicular GABA release[1], enhanced tonic current may be caused by increased vesicular GABA. However, sIPSC frequency, a measure of action–potential dependent vesicular GABA release, was not significantly higher in GAERS compared to NEC at any age tested (**Supplementary Table 1**). Furthermore, miniature IPSC (mIPSC) frequency, recorded in the presence of 0.5 μM TTX, was no different between P18–21 GAERS and NEC (4.3 ± 0.7 Hz and 4.7 ± 0.9 Hz, respectively). Interestingly, similar sIPSC and mIPSC frequencies in each strain indicate that under our experimental conditions the majority of vesicular GABA release is quantal. In agreement with this, we saw no effect of TTX on tonic current amplitude in either GAERS or NEC (**Supplementary Fig. 2a**).

Mis–expression of $sGABA_ARs$ in the extrasynaptic membrane might lead to enhanced tonic current. Since $sGABA_ARs$ in TC neurons contain the γ2 subunit and are susceptible to modulation by benzodiazepines[2–4], we compared the effects of the benzodiazepine flurazepam (5 μM) in P18–21 GAERS and NEC. Flurazepam had no effect on tonic current (**Supplementary Fig. 2a**), but did increase the weighted decay of sIPSCs in both strains (data not shown; both $P < 0.05$). Thus, $sGABA_ARs$ are not displaced in the extrasynaptic membrane of GAERS.

Increased tonic current could also be caused by overexpression of δ subunit–containing extrasynaptic receptors. Therefore, we compared the effects of the δ subunit–selective agonist THIP (100 nM) in P18–21 GAERS and NEC. THIP increased tonic current significantly in both GAERS and NEC (both $P < 0.001$). However, the additional THIP–induced currents in both strains were remarkably similar not only to each other (**Supplementary Fig. 2b**), but also to that observed in normal Wistar rats of comparable age (62.6 ± 11.3 pA) (**Fig. 1e**). Thus, the number of $eGABA_ARs$ is not different between GAERS and NEC.

Low concentrations of endogenous taurine activate $eGABA_ARs$ in TC neurons[5], suggesting that enhanced tonic current could arise due to impaired taurine transport in

GAERS. The taurine transporter inhibitor guanidinoethyl sulfonate (GES, 10 μM) significantly increased tonic current in P18–21 GAERS and NEC (both $P < 0.001$). In both strains, however, the additional GES–induced currents were similar (**Supplementary Fig. 2b**), indicating that aberrant taurine transport does not contribute to enhanced tonic current in GAERS.

Expression and genetic variants of GAT–1

Impaired GAT–1 activity in GAERS may be caused by reduced GAT–1 expression. In western blots, GAT–1 was detected as a ~67 kDa band in both GAERS and NEC, but no difference in protein levels were observed in thalamus or cortex (**Supplementary Fig. 4a**). Furthermore, no difference in GAT–1 immunostaining was observed in the thalamus or neocortex between GAERS and NEC (**Supplementary Fig. 4b**).

The mutations underlying absence seizures in GAERS are polygenic and unknown[6], therefore we tested for possible genetic variants in GAT–1. Analysis of cDNA sequences derived from GAERS revealed a single, silent nucleotide polymorphism (G to A) at position 1109 that appears to represent a strain–dependent difference between GAERS and the Brown Norway rat of the Ensembl genomic database. Furthermore, no genetic variants were observed in GAT–1 cDNAs from stargazer or lethargic. In addition, we tested in cDNAs of GAERS for genetic variants in stargazin and the β4 Ca^{2+} channel subunit, the mutated proteins in stargazer and lethargic mice, respectively. However, no genetic variants were found. Thus, GAT–1 malfunction is not due to reduced expression or genetic variation, and the mutations responsible for absence seizures in stargazer and lethargic mice do not occur in GAERS.

SUPPLEMENTARY DISCUSSION

Tonic $GABA_A$ inhibition and absence seizures in tottering mice

Out of the eight preparations that develop absence seizures (GAERS, stargazer, lethargic, tottering, GAT–1 KO, GHB, THIP [systemic or intra–thalamic] and intra–thalamic NO711), the tottering mice were the only one that did not exhibit enhanced tonic $GABA_A$ inhibition. Such a high degree of consistency across preparations is remarkable, especially given the diverse genetic and pharmacological backgrounds of

the different models investigated. Interestingly, tonic current amplitude in tottering mice was of similar magnitude to that seen in both stargazer and lethargic mice, thus a large tonic current seems to be a feature of the background tottering strain. The effects of the inherently large tonic current may only become apparent when combined with the tottering mutation. For instance, absence seizures may appear only when the inherently large tonic current combines with the selectively compromised excitatory rather than inhibitory synaptic transmission that occurs in TC neurons of tottering mice[7], leading to an overwhelming shift in the balance of excitation and inhibition in favour of inhibition. (Interestingly, a similar mechanism may underlie the GHB induction of seizures, with the proposed $GABA_BR$–dependent facilitation of $eGABA_ARs$ combining with the selective reduction in excitatory neurotransmission in the thalamus resulting from the activation of pre–synaptic $GABA_BRs$[8], leading to an overwhelming increase in both phasic and tonic $GABA_A$ inhibition). Or, given the recent demonstration of recovery of both convulsive and non–convulsive epilepsy phenotypes following the crossbreeding of mice, including tottering, with opposing epilepsy mutations[9], it is possible that the EEG and behavioural effects of a large tonic current in control tottering littermates may be effectively masked by other mutations. Despite these arguments, however, another possible explanation is that thalamic $eGABA_ARs$ are not important for the generation of seizures in tottering mice, and that they arise due to some other cellular pathology, suggesting that multiple mechanisms can give rise to the same behavioural abnormalities in different absence seizure models.

Aberrant phasic $GABA_A$ inhibition in absence seizures and the role of synaptic $GABA_ARs$ in the therapeutic treatment of absence epilepsy

Our data show that phasic inhibition in TC neurons is largely unaltered in the genetic models examined, with the exception of the GAT–1 KO mice where there is an apparent gain–of–function in sIPSCs. This is in agreement with previous studies on sIPSCs in young GAERS[10], in transgenic mice with a mutation (γ2R43Q) identified in an epileptic human cohort[11], and evoked IPSCs in lethargic and tottering mice[7]. However, changes in putative $sGABA_ARs$ have been demonstrated in an acquired model of absence seizures, most notably a reduction of γ2 subunit expression[12], although the functional consequences of this reduction were not examined because

IPSCs were not measured. This general lack of change in phasic inhibition apparently contradicts the fact that absence epilepsy can be successfully treated by the benzodiazepine clonazepam. However, it is has been demonstrated that clonazepam has its action in the nucleus reticularis thalami (NRT) rather than sensory thalamic nuclei, because it selectively targets $GABA_A$Rs containing the α3 subunit that are present in the NRT but not the VB[13–15]. An NRT–specific locus of clonazepam action is supported by its lack of effect on absence seizures when selectively administered to the VB of lethargic mice, whereas intra–NRT administration suppresses seizures[16]. In summary, changes in phasic inhibition in TC neurons are rare in models of absence seizures, whereas our findings show that aberrant tonic inhibition is more prevalent. Furthermore, s$GABA_A$Rs in TC neurons are not a current target for therapy, whereas those in the NRT are.

Aberrant tonic inhibition in other models of epilepsy

Our findings are the first to show enhanced e$GABA_A$R function as a common mechanism in diverse models of generalized epilepsy, and in the case of GAERS prior to the onset of absence seizures. Previous studies have identified aberrant e$GABA_A$R function following the induction of temporal lobe epilepsy, but observed changes are variable and somewhat contradictory. Thus, after pilocarpine induced status epilepticus, tonic $GABA_A$ current is either enhanced[17] or unaltered[18] in DGGCs. Furthermore, tonic current is increased in CA1 pyramidal neurons after pilocarpine or kainic acid administration, but only in the presence of elevated ambient GABA[19], or reduced in cultured pyramidal neurons following chronic treatment with kainic acid or cyclothiazide[20]. Interestingly, in cultured hippocampal neurons from mice with a $GABA_A$R γ2 subunit mutation (R43Q) found in humans with generalized epilepsy including absences[21], tonic current was reduced, but there was no effect in neurons from another γ2 subunit (K289M) mutant mouse strain[22]. Furthermore, a reduction in tonic current has been shown in DGGCs of stargazer[23]. Together with our results, this suggests that cell–type specific changes in e$GABA_A$R function can occur in the same animal. However, in light of these findings in both stargazer and γ2R43Q mice, it is important to bear in mind that the hippocampal formation does not participate in the generation or maintenance of absence seizures, and that both mouse strains have a phenotype more complex than absence seizures alone.

Changes in $GABA_AR$–mediated inhibition have also been documented in two mouse models of autosomal dominant nocturnal frontal lobe epilepsy (ADNFLE)[24], a partial epilepsy syndrome that arises due to mutations in nicotinic ACh receptor subunit genes[25]. In ADNFLE mice, seizures were suppressed by administration of the $GABA_AR$ antagonist picrotoxin, whereas there was negligible effect in WT mice. In cortical neurons, sIPSCs were no different between mutant mice and WTs, but application of nicotine caused a massive increase in sIPSC frequency and amplitude in the mutants that was not apparent in WTs[24]. Although it was not examined, one might expect a concomitant increase in tonic inhibition in response to the nicotine–induced increase in vesicular GABA release.

Aberrant GAT–1 function has also previously been described in models of convulsive epilepsy. In seizure prone rats, audiogenic seizures induced a large reduction in GAT–1 mRNA expression in hippocampus and cortex[26]. Kainic acid–induced seizures compromised GAT–1 function in hippocampus[27], and reduced immunoreactivity of neocortical GAT–1 was observed after pilocarpine administrations. Similarly, GAT–1 immunoreactivity in the dentate gyrus was reduced following kindling evoked seizures[28]. Loss of GAT–1 has been observed in patients with temporal lobe epilepsy[27,29]. However, our data show that impaired GAT–1 function need not necessarily correlate with loss of GAT–1 expression to cause epileptic phenotypes.

A possible role for thalamic $eGABA_ARs$ in absence seizures

Given our current knowledge of thalamo–cortical interactions during absence episodes[30,31], we suggest the following role of enhanced tonic $GABA_A$ inhibition in SWDs. Seizures arise due to paroxysmal development of normal 5–9 Hz oscillations in a discrete somatosensory cortical initiation site[32–34], which powerfully excites the GABAergic neurons of the NRT[35]. These neurons respond by generating low–threshold Ca^{2+} potential–mediated bursts of action potentials on every cycle of the SWD, resulting in barrages of IPSPs in TC neurons which override the cortical excitation[35,36]. Concomitantly, ambient GABA levels increase[37] due to reduced GABA uptake by GAT–1, enhancing $eGABA_AR$ function directly, and indirectly by $GABA_BR$–dependent facilitation. Enhanced tonic inhibition, in combination with classical post-synaptic $GABA_BR$ activation (see below), persistently hyperpolarises

the TC neurons and increases membrane conductance[3], reducing the action potential output of the TC neurons, with low threshold Ca^{2+} potential–mediated bursts of action potentials rarely occurring[36,38,39]. Furthermore, the responsiveness of TC neurons to excitatory, sensory synaptic input is reduced, 'gating' information flow through the thalamus and causing behavioural arrest. The rhythmic IPSP barrages entrain TC neuron output to cycles of the SWD, providing a sparse but synchronised input to the cortex and maintaining paroxysmal activity in the thalamo–cortical network. Whilst our hypothesis focuses on the role of enhanced tonic inhibition in the thalamus, we do not exclude the possibility that other cellular alterations in the thalamo–cortical network, perhaps including increased tonic inhibition in the cortex, may contribute to seizures, and that different cellular mechanisms may underlie absence seizures in different models. Furthermore our hypothesis supports the observation that although SWDs are initiated in the cortex, intact thalamo–cortical networks are required for the full behavioural expression of absence seizures[34].

$GABA_B$ receptors and absence seizures

Our data highlight a potentially novel contribution of $GABA_B$Rs to absence seizures, a $GABA_B$R–dependent facilitation of e$GABA_A$R function. Whilst the mechanism(s) underlying this effect have yet to be determined, they suggest that the $GABA_B$R sensitivity of absence seizures is due, at least in part, to this novel receptor–receptor interaction. Indeed the sensitivity of SWDs to $GABA_B$R modulation is a defining characteristic of absence seizures, and previous studies in both genetic and pharmacological models of absence seizures have shown that systemic or intra–thalamic administration of $GABA_B$R agonists are capable of inducing or exacerbating SWDs, whereas $GABA_B$R antagonists suppress them[40–42]. In addition, absence seizures can be induced following intra–VB administration of GHB[43], a weak agonist at $GABA_B$Rs, although the contribution of a putative GHB receptor cannot be discounted[44]. The apparent $GABA_B$R mediated augmentation of e$GABA_A$R function occurs despite the reduction in GABA release and ambient GABA following activation of pre-synaptic $GABA_B$Rs[45,46].

The novel $GABA_B$R–e$GABA_A$R interaction does not detract from the classical post-synaptic $GABA_B$R effects, i.e. the opening of G protein–coupled inwardly rectifying K^+ channels. In addition to barrages of IPSPs arising from GABAergic NRT neurons,

TC neurons exhibit a persistent hyperpolarization during SWDs[36,47]. Furthermore, eGABA$_A$R and post–synaptic GABA$_B$R activation leads to an increase in membrane conductance[3,48]. Together, these effects cause TC neurons to generate action potentials only rarely during SWDs, but with sufficient synchrony to drive the cortex and maintain seizures[36,38,47]. Our data suggest that the combined effects of eGABA$_A$R activation, post–synaptic GABA$_B$R activation, and GABA$_B$R–dependent facilitation of eGABA$_A$Rs is responsible for the membrane hyperpolarization and increase in membrane conductance. Although one would predict that hyperpolarization of TC neurons should initiate low–threshold Ca^{2+} potential–dependent burst firing[49], this is apparently not case, and, as described above, TC neurons rarely fire any action potentials, let alone bursts, during a SWD[36,38,47]. We suggest that the increase in membrane conductance has greater impact on the responsiveness of TC neurons than the hyperpolarization, effectively preventing the generation of low–threshold Ca^{2+} potential–dependent bursts and making the TC neurons unresponsive to synaptic input. Thus, the silencing of TC neurons during most of the SWD effectively 'gates' the thalamus, and probably underlies the behavioural arrest characteristic of absence seizures. This is in contrast to an *in vitro* model of thalamic hyperexcitability elicited by GABA$_A$R antagonists where GABA$_B$R activation drives burst firing of TC neurons on every cycle of the paroxysmal activity[50–52]. However, absence seizures are suppressed by intra–VB administration of GABA$_A$R antagonists not exacerbated, at least in GAERS[40]. Despite the intimate involvement of GABA$_B$Rs in seizure genesis, they ultimately do not appear to be a target for therapeutic intervention, but may play a role in exacerbation of absence seizures by anti–convulsants such as tiagabine and vigabatrin. In any case, we have potentially identified the cellular mechanisms by which both tiagabine and vigabatrin exacerbate absence seizures.

SUPPLEMENTARY METHODS

In vitro slice preparation and whole–cell patch clamp recordings

Slice preparation and whole–cell patch clamp recordings were performed as described previously[3]. Briefly, male and female Wistars, GAERS, NEC, stargazer, lethargic, tottering and respective control littermates, and GAT–1 and δ subunit KO and respective WT littermates, of the relevant postnatal ages (see text for details) were anaesthetised with isoflurane and decapitated, in accordance with the United

Kingdom Animals (Scientific Procedures) Act 1986 and associated procedures. The brains were rapidly removed, and 300 μm thick horizontal sections containing either the thalamus or hippocampus were cut, using a vibroslicer (HM 650 V, Microm International, Walldorf, Germany), in cold (<4 ºC), continuously oxygenated (95% O_2: 5% CO_2) artificial CSF (aCSF) containing (in mM): NaCl 85, $NaHCO_3$ 26, $MgCl_2$ 2, $CaCl_2$ 2, KCl 2.5, NaH_2PO_4 1.25, glucose 10, sucrose 73.6, indomethacin 0.045, and kynurenic acid 3. Indomethacin and kynurenic acid were included to improve slice viability[3]. Slices were stored in an oxygenated incubation chamber containing the above aCSF, but without indomethacin and kynurenic acid, for 15–20 mins before the aCSF was gradually replaced with aCSF containing (in mM): NaCl 126, $NaHCO_3$ 26, $MgCl_2$ 2, $CaCl_2$ 2, KCl 2.5, NaH_2PO_4 1.25 and glucose 10. Slices were left for at least 1 hr before being transferred to the recording chamber where they were continuously perfused (1.5 ml min^{-1}) with warmed (33 ± 1 ºC), oxygenated aCSF containing (in mM): NaCl 126, $NaHCO_3$ 26, $MgCl_2$ 1, $CaCl_2$ 2, KCl 2.5, NaH_2PO_4 1.25, glucose 10 and kynurenic acid 3. Kynurenic acid was used in the recording medium to isolate $GABA_AR$ currents. Experiments utilising GHB and THIP in Wistar rats *in vitro* were performed in the presence of TTX.

TC neurons of the VB, and DGGCs of the hippocampal formation, were visualised using a Nikon microscope (Eclipse E600FN or FN1, Tokyo, Japan) equipped with a 40× immersion lens and a video camera (Hamamatsu, Hamamatsu City, Japan). Whole cell patch clamp recordings were made from neurons held at –70 mV using pipettes (resistance 2-4 MΩ) containing (in mM): CsCl 130, $MgCl_2$ 2, Mg-ATP 4, Na-GTP 0.3, Na-HEPES 10 and EGTA 0.1, pH 7.25–7.30, osmolality ~290 mOsm. Pipettes were attached to the headstage of either a Multiclamp 700B preamplifier, controlled by Multiclamp Commander software, or an Axopatch 200A preamplifier (Molecular Devices, Sunnyvale, CA, USA). Data were discarded if the series resistance changed by >30%. Experimental data were digitized at 20 kHz (Digidata 1322, Molecular Devices), acquired using pClamp 9.0 software (Molecular Devices), and stored on a personal computer.

Data were filtered at 3 kHz and converted to an ASCII format for analysis using LabView based software (National Instruments, Austin, TX, USA)[3]. The presence of

a tonic $GABA_A$ current was determined using a high concentration of the $GABA_AR$ antagonist gabazine (GBZ). Briefly, tonic currents were observed as an outward shift in baseline current following focal, or in some cases bath, application of 100 μM GBZ, since the holding potential was –70 mV and the reversal potential of Cl^- ~0 mV. To measure tonic current amplitude, 5 ms epochs of baseline current were sampled every 100 ms, and those epochs that fell on IPSCs discarded. The average baseline current was then calculated for two 5 s periods prior to (i and ii), and one after (iii), GBZ application. The background 'drift' of the baseline current was calculated as the difference between the two pre–GBZ periods (ii–i), and the GBZ–dependent 'shift' due to block of the tonic current as the difference between the second pre–GBZ period and the post–GBZ period (iii–ii)[3]. A tonic current was presumed to be present for a given neuron if the post–GBZ shift was twice the standard deviation of the pre–GBZ drift. In some instances, tonic current amplitude was normalised to whole–cell capacitance, which was calculated from small (5 mV) voltage steps before and after experiments. For analysis of IPSCs, populations of individual IPSCs were averaged, and the peak amplitude, charge transfer (the integral of the average IPSC), weighted decay time constant (integral of the average IPSC divided by peak amplitude), frequency, and total current (charge transfer X frequency) measured[3]. Tonic current amplitude and IPSC properties were compared between strains in different populations of recorded neurons. Similarly, the actions of bath applied drugs on tonic current amplitude and IPSC properties were measured in a different population of neurons and then compared to the population of control neurons[3], except for THIP where control and drug action were measured in the same cell. Data from the THIP experiments was analysed by measuring 5 ms epochs of baseline current every 100 ms for three 20 s periods, one prior to wash–on of THIP, one during THIP application, and one following focal application of GBZ. The effects of THIP alone and THIP and GBZ together were then calculated relative to the control period.

GAT–1 western blot analysis

Young adult GAERS and NEC (three each) were killed by cervical dislocation and samples of the cerebral cortex and thalamus rapidly dissected and frozen on dry ice. Total protein was extracted and subjected to western blot analysis using standard

procedures[53]. The primary antibodies used were the GAT–1–specific antibody AB1570W (Chemicon, Millipore Corporation, Billerica, MA, U.S.A.), and the GAPDH–specific antibody ab9485 (Abcam Ltd., Cambridge, U.K.). Protein bands were detected using enhanced chemiluminescence (ECL plus, Amersham/GE Healthcare UK, Little Chalfont, Bucks., U.K.) and quantitated by densitometry (Imagequant^{TM} 3.0, Amersham/GE). Levels of GAT–1 protein were corrected for (extraction and loading) variation against the equivalent GAPDH protein band.

Immunocytochemistry of GAT–1

Male GAERS and NEC (two each, P18–21) were anaesthetised with sodium pentobarbital in accordance with the UK Animals (Scientific Procedures) Act 1986 and associated procedures, and transcardially perfused initially with phosphate–buffered saline (PBS, 0.1 M) followed by 4% paraformaldehyde in PBS for 10 mins. Brains were removed, extensively rinsed with PBS containing 0.2% Tween 20, and coronal sections (50–60 μm) cut on a vibrotome. Sections were incubated in 3% normal goat serum for 1.5 hrs, followed by incubation in rabbit GAT–1–specific antibody (1:600; ab1570, Chemicon) for 2.5 hrs at room temperature, and then overnight at 4 ºC. On the following day, sections were incubated in the secondary antibody (biotinylated goat anti–rabbit, 1:200; Vector Laboratories, Burlingame, CA, U.S.A.) for 2.5 hrs at room temperature, and staining visualised using the avidin–biotin–horseradish peroxidise complex procedure (Vecstatin ABC Elite Kit, Vector Laboratories). Peroxidase enzyme activity was revealed with 3,3'–diaminobenzidine tetrahydrochloride as chromogen and 0.003% H_2O_2 as substrate. The enzyme reaction lasted for 5 mins.

cDNA cloning and sequencing

Young adult GAERS, stargazer and lethargic animals (one each) were killed by cervical dislocation and samples of the cerebellum and thalamus rapidly dissected and frozen on dry ice. Total RNA was extracted and cDNA clones of the GAT–1 coding sequence, and the stargazin and β4 Ca^{2+} channel subunit coding sequences for GAERS, were obtained using standard RT–PCR procedures as described[54]. PCR primer sequences were derived from Ensembl transcripts (http://www.ensembl.org/index.html). Each coding sequence was cloned as multiple

fragments of 400–700 bp and sequenced by the DNA Sequencing Core Laboratory in the Cardiff School of Biosciences (http://watson-bios.grid.cf.ac.uk/seq/default.php). At least two individual clones were sequenced for each fragment and then compared with database mRNA sequences (Ensembl, NCBI; http://www.ncbi.nlm.nih.gov).

EEG recordings and reverse microdialysis in behaving animals

All surgical procedures were performed in accordance with the UK Animals (Scientific Procedures) Act 1986 and associated procedures. Male and female GAT–1 KO (25–35 g, 6–7 months of age), δ KO and WT mice (25–35 g, 6–12 months of age), male Wistar rats (250–300 g, >13 weeks of age), and male GAERS (250–350 g, 6–12 months of age) were anaesthetised with a mixture of isoflurane and N_2O. In Wistar and GAERS animals, six screw electrodes were placed bilaterally over the frontal cortex, parietal cortex and cerebellum, whilst in KO and WT mice only four screws, bilaterally over the parietal cortex and cerebellum, were implanted. Mice underwent no further surgery.

For reverse microdialysis experiments in Wistars two guide cannulae were implanted over the VB thalamus and permanently fixed to the skull with methylacrylic cement. The position of cannulae was checked post hoc (**Fig. 5d**) and data from animals with incorrectly positioned cannulae were not included for further analysis. After one week of recovery, two microdialysis probes (CMA/12, 2 mm length and 500 μm outer diameter; Carnegie Medicin, Stockholm, Sweden) connected to a two-channel liquid swivel (Carnegie Medicin) were inserted down the guide cannulae to a depth 2 mm below the end of the cannulae.

For anti– and missense ODN experiments in GAERS, cannulae were implanted and ODNs injected after one week of recovery. To determine the spread of injected ODNs, we used a biotinylated antisense ODN and staining was visualised using the avidin–biotin–horseradish peroxidase complex procedure (**Fig. 5d**). For *in vitro* experiments measuring tonic current amplitude after ODN injection, P28–32 GAERS were implanted with guide cannulae only, ODNs injected 2 d after surgery, and thalamic slices prepared 22–26 hrs after injection, as above.

During experiments, all animals were transferred to the recording cage, and EEG recordings made using a Neurolog (Digitimer Ltd, Welwyn Garden City, U.K.) or Plexon (model REC/64; Dallas, Texas, U.S.A.) amplifier. Data were analysed using pClamp 9.0 (Molecular Devices) or Plexon software, respectively.

In GAT–1 KO mice, spontaneous SWDs were recorded for a period of 1 hr. Seizures were quantified as the time spent in seizure during 15 min periods. The effect of ETX was tested by i.p. injection of 200 mg kg^{-1} in a volume of 1 ml kg^{-1}.

In δ KO mice and WT littermates, control EEG recordings were made for 15 mins prior to systemic injection of GBL (50 mg kg^{-1} i.p.) and the effects of GBL recorded for 1 hr. Seizures were quantified as the time spent in seizure during 15 min periods, and the effect of ETX was tested by i.p. injection of 200 mg kg^{-1} in a volume of 1 ml kg^{-1}.

In Wistars implanted with reverse microdialysis probes, experiments consisted of three stages. Firstly, a control period (30 mins) was recorded without probes. Secondly, a period of 20 mins was recorded with probes infusing aCSF (1 μl min^{-1}) containing (in mM): 147 Na^+, 2.7 K^+, 1 Mg^{2+}, 1.2 Ca^{2+} and 154.1 Cl^-, adjusted to pH 7.4 with 2 mM sodium phosphate buffer. Thirdly, a period of 120 mins was recorded with probes infusing either aCSF alone or aCSF containing NO711 (200 μM) or THIP (30–100 μM). A technical drawback of reverse microdialysis is that it reduces the effective concentration of administered drug to =10% (ref. 55). Therefore the final concentration of NO711 was likely to be =20 μM, i.e. still selective for GAT–1 (ref. 56), and the final concentration of THIP was likely to be =7–10 μM, i.e. still selective for e$GABA_A$Rs[57]. Seizures were quantified as the time spent in seizure during 20 min periods, and the total number of SWDs was also calculated. The effects of ETX were tested by i.p. injection of 100 mg kg^{-1} in a volume of 1 ml kg^{-1}.

For anti– and missense experiments in GAERS, control recordings were made for 1 hr prior to the injection of ODNs, and experiments started 1 d after injection. Seizures were quantified as the time spent in seizure during 1 hr periods and normalized to the control recordings. The total number of SWDs was also calculated.

During the recording session, all animals were gently stimulated to prevent them falling asleep if required, and video monitored to record the behavioural components of absence seizures.

Drug effects were assessed by repeated measures ANOVA with post–hoc Tukey HSD when significant differences were found ($P < 0.05$). The effects of ETX on GBL–, NO711– and THIP–induced seizures were compared using Student's paired t–test ($P < 0.05$).

Sources of animals, and genotyping of mutant mice

Colonies of GAERS and NEC were maintained at the School of Biosciences, Cardiff University. Breeding pairs of stargazer, lethargic, tottering and δ KO mice were obtained from The Jackson Laboratory (Bar Harbor, Maine, U.S.A.), GAT–1 KO mice from the Mutant Mouse Regional Resource Center (University of California, Davis, U.S.A.), and colonies initiated at the School of Biosciences. Wistar rats were obtained from Harlan U.K. Ltd (Bicester, Oxon, U.K.).

Heterozygous breeding pairs of stargazer, lethargic, tottering, GAT–1 KO and δ subunit KO mice were used to generate WT, heterozygous and mutant offspring. For the majority of experiments, stargazer, lethargic and tottering mutant mice were identified by their ataxic phenotypes[58] and compared to control littermates, i.e. WT and heterozygous mice since the stargazer, lethargic and tottering mutations are recessive. For experiments in pre–seizure stargazer, lethargic and tottering mice, animals could not be identified by phenotype, therefore conventional genotyping protocols involving PCR amplification of genomic DNA were used. The oligonucleotide primers used to identify stargazer mice were: STAR–3 5'–ACT GTC ACT CTA TCT GGA ATC–3', LTR–5 5'–GAG CAA GCA GGT TTC AGG C–3', LTR–3 5'–GCC TTG ATC AGA GTA ACT GTC–3' and STAR–5 5'–CAT TTC CTG TCT CAT CCT TTG–3', giving rise to bands of 600 bp in WT, 600, 300 and 400 bp in heterozygous, and 300 and 400 bp in stargazer mice. The primers used to identify lethargic mice were: Leth–5 5'–AAA TGG TAT CAG GAA CAT TCC GAG C–3' and Leth–3 5'–CAA ACC AGT GAA AGC GTT AGC AAG C–3' giving rise

to bands of 75 bp in WT, 75 and 79 bp in heterozygous and 79 bp in lethargic mice. The primers used to identify tottering mice were: IMR 1949 5'–AAC CTG GTT GTC TCC CTC CT–3', IMR 1950 5'–TGT CGA AGT TGG TGG GCG–3' and IMR 1951 5'–TGT CGA AGT TGG GCA–3' giving rise to a band of 665 bp in WT and heterozygous mice when IMRs 1949 and 1950 were combined, and in heterozygous and tottering mice when IMRs 1949 and 1951 were combined. Although GAT–1 KO mice have a phenotype that includes ataxia and tremor[59,60], we genotyped animals in order to identify heterozygous and WT littermates, since the GAT–1 mutation is not recessive. The primers used were: mGAT1 17399–430 5'–GAC ATT TGG CTT ACT AGT GAG GAA ACA AGA GC–3', mGAT1 17830–799 5'–GCT AAG GGG CCT CTA CGG AAG CCT CCA GAG GC–3', and GFP37 9955–64 5'–CCA TCT AAT TCA ACA AGA ATT GGG ACA ACT CC–3' giving rise to bands of 245 bp in GAT–1 KO, 245 and 430 bp in heterozygous, and 430 bp in WT mice. Since δ subunit KO mice exhibit no discernible gross phenotype[61,62], we used genotyping protocols to identify all offspring. The primers used were: DF 5'–ATG ACT GTG TTC CTG CAT CA–3', DR 5'–AGC CCC TCC CTG AAA GCT AG–3', and NCR 5'–TTG TCT GTT GTG CCC AGT CA–3', giving bands of 350 bp in WT, 550 and 1450 bp in δ KO, and 350, 550 and 1450 bp in heterozygous mice. In experiments, GAT–1 and δ KO animals were compared to WT littermates only.

$GABA_AR$ d subunit antisense and missense ODNs

The rat δ subunit–specific antisense ODN was based on that previously used in the mouse[63], and did not show any significant homology to any other sequence in GenBank. The sequence was: CGT TTA TAC CTT ATG TGG TA and differed from that described for the mouse by a single base, as dictated by the cDNA sequence (accession number NM_017289). A missense ODN of identical length was used, and also based on that previously described[63], with no significant homology to any other sequence in GenBank. The missense sequence was: ATG GTA TAT TCC ATG TTT GC. For localization of injected ODN spread (**Fig. 5d**) a 3' biotin–modified antisense ODN, with the same sequence as above, was used. Antisense and missense ODNs were obtained from Sigma-Genosys Ltd (Cambridge, U.K.).

Sources of drugs

Drugs were obtained from the following sources: kynurenic acid, 4,5,6,7–tetrahydroisoxazolo–[5,4–C]pyridine–3–ol (THIP), γ–hydroxybutyric acid (GHB), 1–(2–[([diphenylmethylene]imino)–oxy]ethyl)–1,2,5,6–tetrahydro–3–pyri–dinecarboxylic acid hydrochloride (NO711), 7–chloro-1–(diethylamino)ethyl–5–(2–fluorophenyl)–3H–1,4–benzodiazepin–2(1H)–one (flurazepam), γ–butyrolactone (GBL), 2–ethyl–2–methylsuccinimide (ethosuximide), sodium 2–propylpentanoate (sodium valproate), and 3,3'–diaminobenzidine tetrahydrochloride from Sigma–Aldrich (Poole, Dorset, U.K.); 6–imino–3–(4–methoxyphenyl)–1–(6H)–pyridazinebutanoic acid hydrobromide (gabazine), (2*S*)–3–[[(1*S*)–1–(3,4–dichlorophenyl)ethyl]amino–2–hydroxypropyl]–(phenylmethyl) phosphinic acid (CGP55845), tetrodotoxin (TTX), 1–[2[*tris*(methoxyphenyl)methoxy]ethyl]–(*S*)–3–piperidinecarboxylic acid ((*S*)–SNAP5114) and 6,7,8,9–tetrahydro–5–hydroxy–5*H*–benzocyclohept–6–ylideneacetic acid (NCS–382) from Tocris Bioscience (Bristol, U.K.); guanidinoethyl sulfonate (GES) from Toronto Research Chemicals Inc. (North York, ON, Canada). All drugs were dissolved directly in aCSF, with the exception of CGP55845 and SNAP5114 which were initially dissolved in DMSO before addition to the aCSF. For *in vitro* experiments NO711 was dissolved in DMSO, for reverse microdialysis experiments in aCSF.

SUPPLEMENTARY REFERENCES

1. Bright, D.P., Aller, M.I. & Brickley, S.G. Synaptic release generates a tonic $GABA_A$ receptor-mediated conductance that modulates burst precision in thalamic relay neurons. *J. Neurosci.* **27**, 2560-2569 (2007).
2. Belelli, D., Peden, D.R., Rosahl, T.W., Wafford, K.A. & Lambert, J.J. Extrasynaptic $GABA_A$ receptors of thalamocortical neurons: a molecular target for hypnotics. *J. Neurosci.* **25**, 11513-11520 (2005).
3. Cope, D.W., Hughes, S.W. & Crunelli, V. $GABA_A$ receptor-mediated tonic inhibition in thalamic neurons. *J. Neurosci.* **25**, 11553-11563 (2005).
4. Jia, F. *et al*. An extrasynaptic $GABA_A$ receptor mediates tonic inhibition in thalamic VB neurons. *J. Neurophysiol.* **94**, 4491-4501 (2005).
5. Jia, F. *et al*. Taurine is a potent activator of extrasynaptic $GABA_A$ receptors in the thalamus. *J. Neurosci.* **28**, 106-115 (2008).

6. Rudolf, G. *et al*. Polygenic control of idiopathic generalized epilepsy phenotypes in the genetic absence rats from Strasbourg (GAERS). *Epilepsia* **45**, 301-308 (2004).
7. Caddick, S.J. *et al*. Excitatory but not inhibitory synaptic transmission is reduced in lethargic (*Cacnb4*^{lh}) and tottering (*Cacna1a*^{tg}) mouse thalami. *J. Neurophysiol.* **81**, 2066-2074 (1999).
8. Gervasi, N. *et al*. Pathway specific action of γ-hydroxybutyric acid in sensory thalamus and its relevance to absence seizures. *J. Neurosci.* **23**, 11469-11478 (2003).
9. Glasscock, E., Qian, J., Woo, J.W. & Noebels, J.L. Masking epilepsy by combining two epilepsy genes. *Nat. Neurosci.* **10**, 1554-1558 (2007).
10. Bessaïh, T. *et al*. Nucleus-specific abnormalities of GABAergic synaptic transmission in a genetic model of absence seizures. *J. Neurophysiol.* **96**, 3074-3081 (2006).
11. Tan, H.O. *et al*. Reduced cortical inhibition in a mouse model of familial childhood absence epilepsy. *Proc. Natl. Acad. Sci. USA* **104**, 17536-17541 (2007).
12. Li, H., Kraus, A., Wu, J., Huguenard, J.R. & Fisher, R.S. Selective changes in thalamic and cortical $GABA_A$ receptor subunits in a model of acquired absence epilepsy in the rat. *Neuropharmacology* **51**, 121-128 (2006).
13. Browne, S.H. *et al*. Kinetic and pharmacological properties of $GABA_A$ receptors in single thalamic neurons and $GABA_A$ receptor subunit expression. *J. Neurophysiol.* **86**, *2312-2322* (2001).
14. Sohal, V.S., Keist, R., Rudolph, U. & Huguenard, J.R. Dynamic $GABA_A$ receptor subtype-specific modulation of the synchrony and duration of thalamic oscillations. *J. Neurosci.* **23**, 3649-3657 (2003).
15. Badiu, C-I. Sensitivity of thalamic GABAergic currents to clonazepam does not differ between control and genetic absence epilepsy rats. *Brain. Res.* **1026**, 261-266 (2004).
16. Hosford, D.A., Wang, Y. & Cao, Z. Differential effects mediated by $GABA_A$ receptors in thalamic nuclei in *lh*/*lh* model of absence seizures. *Epilepsy Res.* **27**, 55-65 (1997).

17. Naylor, D.E., Liu, H. & Wasterlain, C.G. Trafficking of $GABA_A$ receptors, loss of inhibition, and a mechanism for pharmacoresistance in status epilepticus. *J. Neurosci.* **25**, 7724-7733 (2005).
18. Zhang, N., Wei, W., Mody, I. & Houser, C.R. Altered localization of $GABA_A$ receptor subunits on dentate granule cell dendrites influences tonic and phasic inhibition in a mouse model of epilepsy. *J. Neurosci.* **27**, 7520-7531 (2007).
19. Scimemi, A., Semyanov, A., Sperk, G., Kullmann, D.M. & Walker, M.C. Multiple and plastic receptors mediate tonic $GABA_A$ receptor currents in the hippocampus. *J. Neurosci.* **25**, 10016-10024 (2005).
20. Qi, J-s., Yao, J., Fang, C., Luscher, B. & Chen, G. Downregulation of tonic GABA currents following epileptogenic stimulation of rat hippocampal cultures. *J. Physiol.* **577**, 579-590 (2006).
21. Wallace, R.H. *et al*. Mutant $GABA_A$ receptor γ2-subunit in childhood absence epilepsy and febrile seizures. *Nat. Genet.* **28**, 49-52 (2001).
22. Eugène, E. *et al*. $GABA_A$ receptor γ2 subunit mutations linked to human epileptic syndromes differentially affect phasic and tonic inhibition. *J. Neurosci.* **27**, 14108-14116 (2007).
23. Payne, H.L. *et al*. Aberrant $GABA_A$ receptor expression in the dentate gyrus of the epileptic mutant mouse stargazer. *J. Neurosci.* **26**, 8600-8608 (2006).
24. Klaassen, A. *et al*. Seizures and enhanced cortical GABAergic inhibition in two mouse models of human autosomal dominant nocturnal frontal lobe epilepsy. *Proc. Natl. Acad. Sci. USA* **103**, 19152-19157 (2006).
25. Phillips, H.A. *et al*. Localization of a gene for autosomal dominant nocturnal frontal lobe epilepsy to chromosome 20q13.2. *Nat. Genet.* **10**, 117-118 (1995).
26. Akbar, M.T., Rattray, M., Williams, R.J., Chong, N.W.S. & Meldrum, B.S. Reduction of GABA and glutamate transporter messenger RNAs in the severe-seizure genetically epilepsy-prone rat. *Neuroscience* **85**, 1235-1251 (1998).
27. Patrylo, P.R., Spencer, D.D. & Williamson, A. GABA uptake and heterotransport are impaired in the dentate gyrus of epileptic rats and humans with temporal lobe sclerosis. *J. Neurophysiol.* **85**, 1533-1542 (2001).
28. Sayin, U., Osting, S., Hagen, J., Rutecki, P. & Sutula, T. Spontaneous seizures and loss of axo-axonic and axo-somatic inhibition induced by repeated brief seizures in kindled rats. *J. Neurosci.* **23**, 2759-2768 (2003).

29. During, M.J., Ryder, K.M. & Spencer, D.D. Hippocampal GABA transporter function in temporal-lobe epilepsy. *Nature* **376**, 174-177 (1995).
30. Crunelli, V. & Leresche, N. Childhood absence epilepsy: genes, channels, neurons and networks. *Nat. Rev. Neurosci.* **3**, 371-382 (2002).
31. Blumenfeld, H. Cellular and network mechanisms of spike-wave seizures. *Epilepsia* **46** (Suppl. 9), 21-33 (2005).
32. Meeren, H.K.M., Pijn, J.M., Van Luijtelaar, E.L.J.M., Coenen, A.M.L. & Lopes da Silva, F.H. Cortical focus drives widespread corticothalamic networks during spontaneous absence seizures in rats. *J. Neurosci.* **22**, 1480-1495 (2002).
33. Pinault, D., Slézia, A. & Acsády, L. Corticothalamic 5-9 Hz oscillations are more pro-epileptogenic than sleep spindles in rats. *J. Physiol.* **574**, 209-227 (2006).
34. Polack, P-O. *et al*. Deep layer somatosensory cortical neurons initiate spike-and-wave discharges in a genetic model of absence seizures. *J. Neurosci.* **27**, 6590-6599 (2007).
35. Slaght, S.J., Leresche, N., Deniau, J-M., Crunelli, V. & Charpier, S. Activity of thalamic reticular neurons during spontaneous genetically determined spike and wave discharges. *J. Neurosci.* **22**, 2323-2334 (2002).
36. Pinault, D. *et al*. Intracellular recordings in thalamic neurons during spontaneous spike and wave discharges in rats with absence epilepsy. *J. Physiol.* **509**, 449-456 (1998).
37. Richards, D.A., Lemos, T., Whitton, P.S. & Bowery, N.G. Extracellular GABA in the ventrolateral thalamus of rats exhibiting spontaneous absence epilepsy: a microdialysis study. *J. Neurochem.* **65**, 1674-1680 (1995).
38. Steriade, M. & Contreras, D. Relations between cortical and thalamic cellular events during transition from sleep patterns to paroxysmal activity. *J. Neurosci.* **15**, 623-642 (1995).
39. Steriade, M. & Contreras, D. Spike-wave complexes and fast components of cortically generated seizures. I. Role of neocortex and thalamus. *J. Neurophysiol.* **80**, 1439-1455 (1998).
40. Danober, L., Deransart, C., Depaulis, A., Vergnes, M. & Marescaux, C. Pathophysiological mechanisms of genetic absence epilepsy in the rat. *Prog. Neurobiol.* **55**, 27-57 (1998).

41. Aizawa, M., Ito, Y. & Fukuda, H. Pharmacological profiles of generalized absence seizures in lethargic, stargazer and γ-hydroxybutyrate-treated model mice. *Neurosci. Res.* **29**, 17-25 (1997).
42. Snead, III O.C. Evidence for $GABA_B$-mediated mechanisms in experimental generalized absence seizures. *Eur. J. Pharmacol.* **213**, 343-349 (1992).
43. Snead, III O.C. The γ-hydroxybutyrate model of absence seizures: correlation of regional brain levels of γ-hydroxybutyric acid and γ-butyrolactone with spike wave discharges. *Neuropharmacology* **30**, 161-167 (1991).
44. Andriamampandry, C. *et al*. Cloning and characterization of a rat brain receptor that binds the endogenous neuromodulator γ-hydroxybutyrate (GHB). *FASEB Journal* **17**, 1691-1693 (2003).
45. Banerjee, P. K. & Snead III, O.C. Presynaptic *gamma*-hydroxybutyric acid (GHB) and *gamma*-aminobutyric $acid_B$ ($GABA_B$) receptor-mediated release of GABA and glutamate (GLU) in rat thalamic ventrobasal nucleus (VB): a possible mechanism for the generation of absence-like seizures induced by GHB. *J. Pharm. Exp. Ther.* **273**, 1534-1543 (1995).
46. Le Feuvre, Y., Fricker, D. & Leresche, N. $GABA_A$ receptor-mediated IPSCs in rat thalamic sensory nuclei : patterns of discharge and tonic modulation by GABAB autoreceptors. *J. Physiol.* **502**, 91-104 (1997).
47. Charpier, S. *et al*. On the putative contribution of $GABA_B$ receptors to the electrical events occurring during spontaneous spike and wave discharges. *Neuropharmacology* **38**, 1699-1706 (1999).
48. Williams, S.R., Turner, J.P. & Crunelli, V. Gamma-hydroxybutyrate promotes oscillatory activity of rat and cat thalamocortical neurons by a tonic $GABA_B$ receptor-mediated hyperpolarization. *Neuroscience* **66**, 133-141 (1995).
49. Jahnsen, H. & Llinás, R. Electrophysiological properties of guinea-pig thalamic neurones: an *in vitro* study. *J. Physiol.* **349**, 205-226 (1984).
50. von Krosigk, M., Bal, T. & McCormick, D.A. Cellular mechanisms of a synchronized oscillation in the thalamus. *Science* **261**, 361-364 (1993).
51. Bal, T., von Krosigk, M. & McCormick, D.A. Synaptic and membrane mechanisms underlying synchronized oscillations in the ferret lateral geniculate nucleus *in vitro*. *J. Physiol.* **483**, 641-663 (1995a).

52. Bal, T., von Krosigk, M. & McCormick, D.A. Role of ferret perigeniculate nucleus in the generation of synchronised oscillations *in vitro*. *J. Physiol.* **483**, 665-685 (1995b).
53. Smith, M. *et al*. Tissue-specific transgenic knock-down of Fos related antigen-2 (Fra-2) expression mediated by a dominant negative Fra-2. *Mol. Cell. Biol.* **21**, 3704-3713 (2001).
54. Holter, J., Davies, J., Leresche, N., Crunelli, V. & Carter, D.A. Identification of two further splice variants of *GABABR1* characterises the conserved micro-exon 4 as a hotspot for regulated splicing in the rat brain. *J. Mol. Neurosci.* **26**, 99-108 (2005).
55. Juhász, G., Kékesi, K., Emri, Zs., Soltesz, I. & Crunelli, V. Sleep-promoting action of excitatory amino acid antagonists: a different role for thalamic NMDA and non-NMDA receptors. *Neurosci. Letts.* **114**, 333-338 (1990).
56. Borden, L.A. GABA transporter heterogeneity: pharmacology and cellular localization. *Neurochem. Int.* **29**, 335-356 (1996).
57. Stórustovu, S. & Ebert, B. Pharmacological characterization of agonists at δ-containing $GABA_A$ receptors: functional selectivity for extrasynaptic receptors is dependent on the absence of γ2. *J. Pharm. Exp. Ther*. **316**, 1351-1359 (2006).
58. Fletcher, C.F. & Frankel, W.N. Ataxic mouse mutants and molecular mechanisms of absence epilepsy. *Hum. Mol. Genet.* **8**, 1907-1912 (1999).
59. Chiu, C-S. *et al*. GABA transporter deficiency causes tremor, ataxia, nervousness, and increased GABA-induced tonic conductance in cerebellum. *J. Neurosci.* **25**, 3234-3245 (2005).
60. Cai, Y-Q. *et al*. Mice with genetically altered GABA transporter subtype I (*GAT1*) expression show altered behavioural responses to ethanol. *J. Neurosci. Res.* **84**, 255-267 (2006).
61. Mihalek, R.M. *et al*. Attenuated sensitivity to neuroactive steroids in γ-aminobutyrate type A receptor delta subunit knockout mice. *Proc. Natl. Acad. Sci. USA* **96**, 12905-12910 (1999).
62. Spigelman, I. *et al*. Behaviour and physiology of mice lacking the $GABA_A$-receptor δ subunit. *Epilepsia* **43** (Suppl. 5), 3-8 (2002).

63. Maguire, J.L., Stell, B.M., Rafizadeh, M. & Mody, I. Ovarian cycle-linked changes in $GABA_A$ receptors mediating tonic inhibition alter seizures susceptibility and anxiety. *Nat. Neurosci.* **8**, 797-804 (2005).